Abyssal Hills and Abyssal Plains

Marie-Helene Cormier and Heather Sloan

Abstract Abyssal hills and abyssal plains makeup the majority of the seafloor, and thus cover vast amount of the Earth's surface. Abyssal hills form in the young oceanic lithosphere near mid-ocean ridges. These elongate, ridge-parallel hills and intervening valleys provide the characteristic fabric of the recently accreted and sparsely sedimented seafloor. Near-bottom investigations document that abyssal hills owe most of their morphology to extensional faulting. Their tectonically-driven growth continues as far as $\sim$35 km from the spreading axis, thus defining a broader plate boundary zone within which the parting plates acquire their steady-state motion. Abyssal hill morphology is sensitive to key aspects of seafloor accretion, and thus preserves accurate records of changing spreading rate, lithospheric thermal structure, and plate boundary geometry. In general, the slower the spreading rate, the larger their dimensions are. This relationship is modulated by regional variations in the thermal structure of the lithosphere, such as may be produced by proximity to hot spots, cold spots, or transform faults and non-transform ridge offsets. As divergent plate motion rafts the aging, subsiding oceanic lithosphere away from the mid-ocean ridge, abyssal hills are generally slowly buried beneath layers of sediments. However, extreme variability in sedimentation rates means that the burial of abyssal hills by sediments is not predictably related to the age of the lithosphere. In fact, the rugged fabric of the abyssal hills is transformed into the remarkably flat surface of the abyssal plains only where oceanic basins are within reach of the fast-moving turbidity currents that originate along the continental margins.

M.-H. Cormier (✉)
Graduate School of Oceanography, University of Rhode Island, Narragansett, RI 02882, USA
e-mail: mhcormier@uri.edu

H. Sloan
Lehman College, City University of New York,
250 Bedford Park Blvd West, Bronx, NY 10468, USA
e-mail: heather.sloan@lehman.cuny.edu

A. Micallef et al. (eds.), *Submarine Geomorphology*, Springer Geology,
DOI 10.1007/978-3-319-57852-1_20

1 Abyssal Hills

Aligned sub-parallel to spreading centers, the repetitive pattern of elongate abyssal hills and intervening valleys creates the distinctive fabric of the young seafloor (Figs. 1 and 2). They were first detected in the mid-twentieth century thanks to the advent of sonar technology (Heezen et al. 1959). As more of the seafloor was ensonified, it became apparent that abyssal hills were a product of seafloor spreading and a ubiquitous feature of the younger oceanic crust. Abyssal hills are often introduced as the most common morphological feature on Earth's surface (Menard 1964; Macdonald et al. 1996; Goff et al. 2004; Buck et al. 2005).

Early near-bottom sonar instruments and direct observations from submersible documented the interplay of normal faulting and volcanism that results in abyssal hill relief (Luyendyk 1970; Rea 1975; Lonsdale 1977; Macdonald and Luyendyk 1985). Later, emerging swath (multibeam) sonar systems produced the first detailed bathymetric maps with a resolution similar to that of land-based topographic maps, revealing the full three-dimensionality of these features (Goff 1992). As data coverage of the ridge flanks continues to expand, so does our understanding of abyssal hill morphology. Many questions about the formation and evolution of abyssal hills remain unsolved or debatable.

This chapter summarizes decades of investigations on abyssal hills and presents a consensus understanding of how spreading rates, lithosphere thermal structure, and changing plate boundary geometry combine to define the varying characteristics of abyssal hills.

1.1 Abyssal Hills Are Shaped by Extensional Tectonics

Direct visual observations, side-scan sonar imagery, and swath bathymetry have established that abyssal hill relief results primarily from slip on normal (extensional) faults (Macdonald 1982; Searle et al. 1984; Macdonald et al. 1996; Goff 2015; Olive et al. 2015). Normal faults initiate about 2-3 km from the axis of accretion, regardless of spreading rates (Macdonald et al. 1982; Searle 1984). Fault length and fault throw (vertical component of slip) continue to increase with distance from the ridge axis for at least 35 km (Alexander and Macdonald 1996; Sloan and Patriat 2004a). This distance is consistent with the broad region of seismicity that surrounds the mid-ocean ridge (Smith et al. 2003). Abyssal hills are therefore produced by a system of interconnected steeply- to moderately-dipping normal faults that continue to accumulate slip up to tens of kilometers away from the ridge axis. Their ultimate morphology thus represents an integrated response to processes that occurred within the broad (at least 70 km-wide) plate boundary zone.

Several tectonic models (Fig. 3) account for the variable morphology of abyssal hills, each one applicable to a particular region (see Goff 1991 and Macdonald et al. 1996 for reviews, and Sauter et al. 2013 for the definition of a new class of abyssal

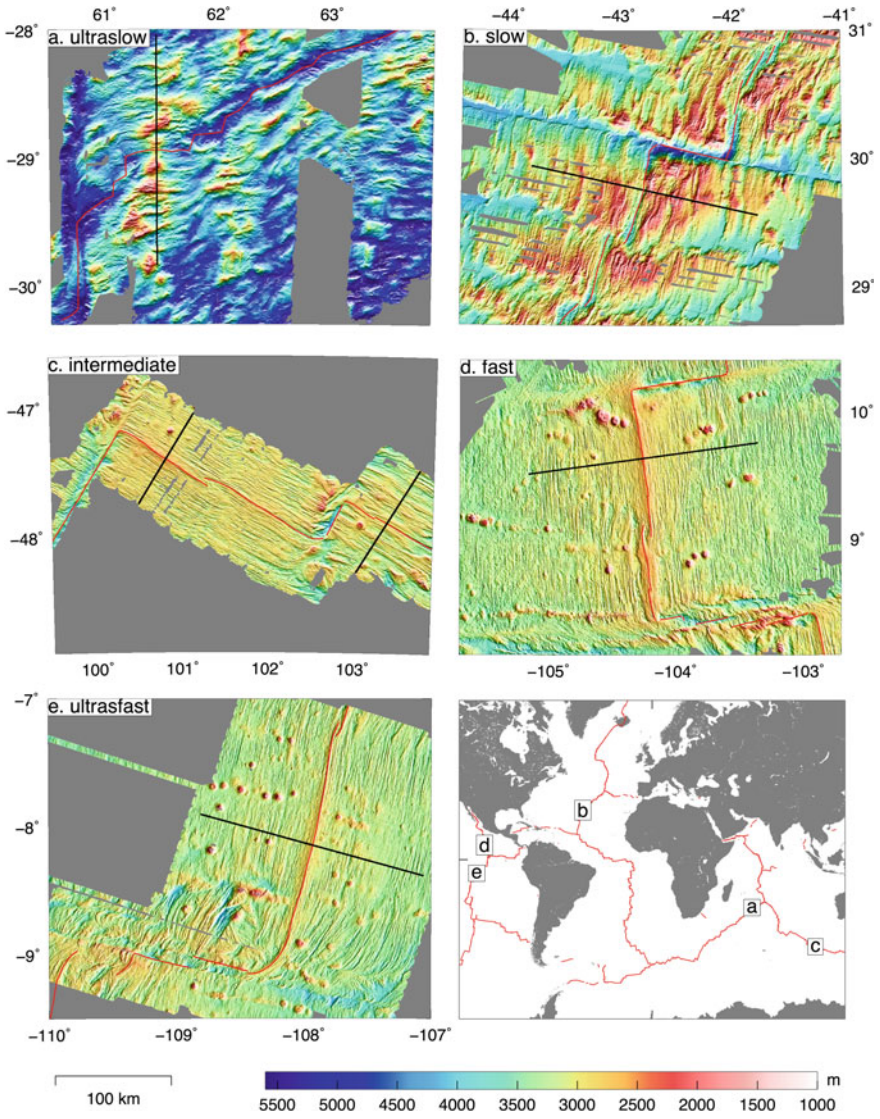

Fig. 1 Five bathymetric maps displaying representative examples of abyssal hill morphology formed at a range of spreading rates, from **a** ultraslow to **e** ultrafast. *Thin red lines* mark the spreading axes and transform faults. *Black lines* locate the bathymetric profiles displayed in Fig. 2. *Index map* at bottom right shows the locations of these five examples

hills). Most models distinguish between "inward-dipping" normal faults, those producing scarps that face toward the spreading center, versus "outward-dipping" faults (those producing scarps that face away from the spreading centers). In the most classic model abyssal hills are the results of "horst and graben" tectonics

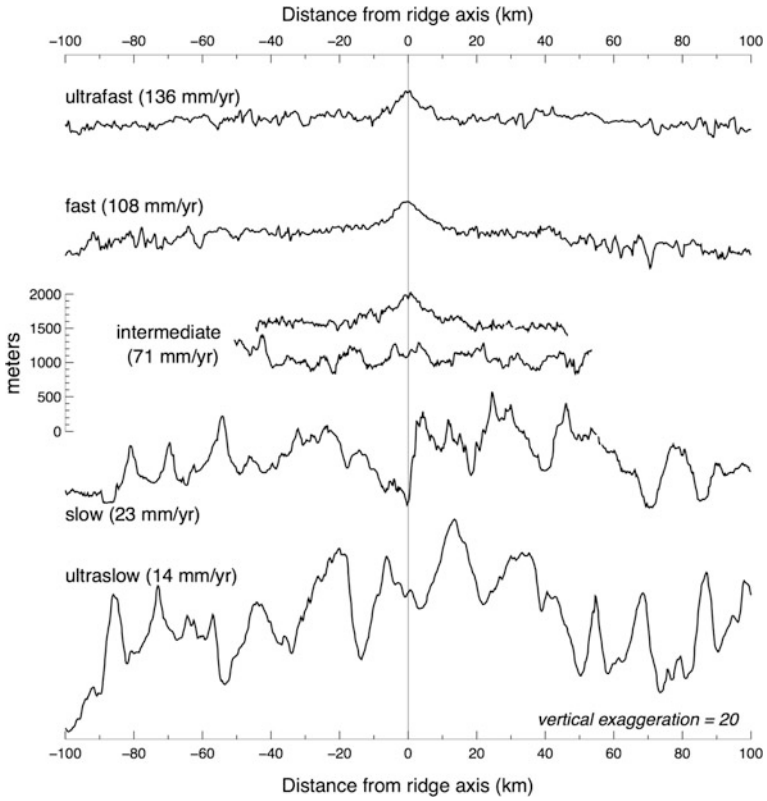

Fig. 2 Bathymetric profiles across the long axis of abyssal hills for a representative range of spreading rates, from ultrafast (*top*) to ultraslow (*bottom*). Profiles are located with black lines in Fig. 1. All profiles are displayed at the same scale with a vertical exaggeration of 20:1. Note the similarity of the top three profiles, all of which correspond to spreading centers marked by an axial high, from intermediate to ultrafast spreading rates. This is in contrast to the variability of the bottom three profiles, which correspond to spreading centers marked by a rifted axis, from ultra-slow to intermediate spreading rates

(Fig. 3a), with each individual hill bounded by an inward-dipping fault and an outward-dipping fault. For fast and intermediate spreading ridges where the spreading axis corresponds to a 15–20 km-wide axial high (see Chapter "Mid-Ocean Ridges"; Figs. 1 and 2), lavas erupting from the summit area may flow outward for long distances and repeatedly drape over nascent outward-dipping fault scarps; where lavas reach the base of the axial high, their flow is dammed by inward-dipping scarps bounding the youngest abyssal hills, thus reducing vertical relief (Fig. 3b). In this case, outward-dipping faults are known as "volcanic growth faults" (Macdonald et al. 1996) and might account for the somewhat gentler slope on the outward-facing side of abyssal hills compared to the inward-facing side

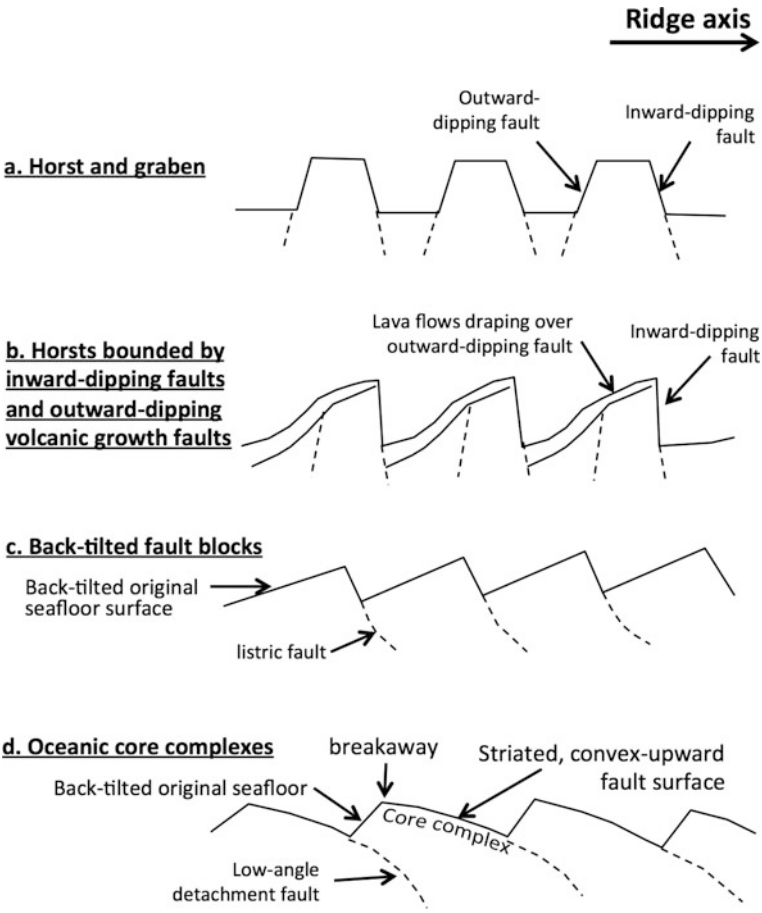

Fig. 3 Four models for the development of abyssal hills. All four models imply the existence of extensional faults that dip toward the ridge axis (inward-dipping) and/or away from the ridge axis (outward-dipping). **a** Horst and graben terrain resulting from inward- and outward-dipping normal faults forming episodically off-axis; **b** Horsts bounded by inward-dipping normal faults and by outward-dipping normal faults that are partly draped by lava flows issued from the ridge axis (volcanic growth faults); **c** Back-tilted fault blocks forming by horizontal axis rotation on inward-dipping normal faults; **d** Oceanic core complex forming through inward-dipping low-angle detachment faults. Detachment fault displays a convex-upward profile, suggesting that rotation of the slip plane occurs as isostatic uplift takes place as a result of prolonged extension on that detachment fault. Modified from Macdonald et al. (1996) and Cann et al. (1997)

(Fig. 4c). Other models may explain marked asymmetries between the inward-facing and outward-facing flanks of abyssal hills. Inward-dipping faults may be listric faults, meaning that the fault surface flattens with depth. Listric faulting results in the outward rotation, or back-tilting, of the intervening fault blocks. In such cases, the back-tilted seafloor constitutes the outward flanks of

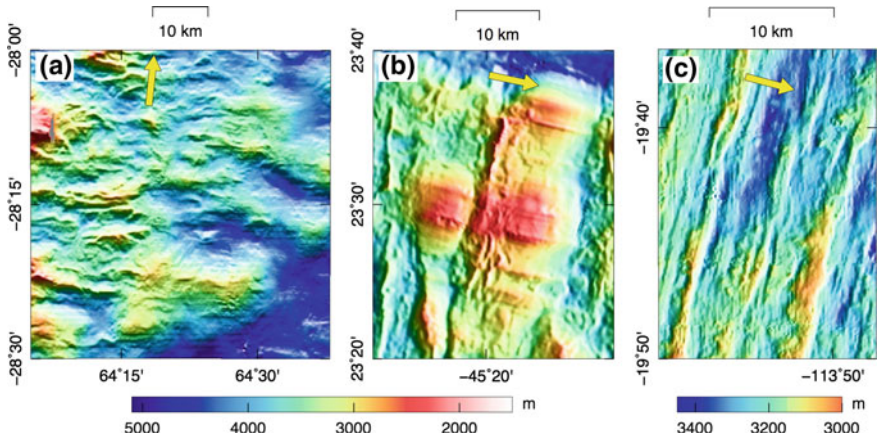

Fig. 4 Shaded-relief bathymetric maps illustrating three styles of abyssal hills. *Yellow arrows* point in the direction of the spreading centers. Different scales and different color scales apply to each map. **a** Abyssal hills formed at the ultraslow-spreading Southwest Indian Ridge. Abyssal hills on the west side are bounded by both inward- and outward-dipping linear fault scarps, and hummocky volcanic features such as cones are recognizable in places. In contrast, abyssal hills on the east side display a smooth relief consisting of broader ridges with rounded profiles ("smooth seafloor"). These hills lack any volcanic texture and, accordingly, almost exclusively mantle-derived rocks have been sampled from their surfaces. **b** Oceanic core complexes formed at the slow-spreading Mid-Atlantic Ridge. Subtle spreading-parallel striations mark the domed surface of the exhumed detachment fault. **c** Abyssal hills formed at the fast-spreading East Pacific Rise. Inward-dipping and outward-dipping linear fault scarps bound individual abyssal hills, with the outward-facing scarps being overprinted in places by lava lobes ("volcanic growth faults")

abyssal hills (Fig. 3c). Occasionally, the inward-facing side and the top surface of an abyssal hill is produced by a large detachment fault (Fig. 3d), known as an oceanic core complex (Cann et al. 1997). In this case, the shallow-dipping fault plane is exhumed over up to tens of kilometers and is marked in plan-view by subtle ridge-perpendicular striations produced by asperities on the fault interface (Fig. 4b). In profile-view, these exhumed fault surfaces are convex-upward and can produce kilometer-scale vertical relief. The steeper outward-facing sides of oceanic core complexes correspond to the original seafloor surface that has been back-tilted by as much as 30°–40° (MacLeod et al. 2009).

While abyssal hills are a product of extensional tectonics within the broader plate boundary zone, their detailed characteristics are modulated by variations in the thermal structure of the lithosphere, spreading rates, and ridge segmentation.

1.2 Influence of the Thermal Structure of the Lithosphere

Although no more than approximately 10% of the oceans has been mapped with high-resolution multibeam bathymetric sonar, existing data are sufficient to outline

some marked regional variations in the morphological characteristics of abyssal hills. The heights of abyssal hill vary by an order of magnitude, from ~50 to >1000 m, and their widths range from ~2 to >10 km (Macdonald and Luyendyk 1985; Goff 1991; Goff et al. 1995, 1997; Cochran et al. 1997; Sauter et al. 2011; Sloan et al. 2012).

This morphological variability primarily reflects regional variations in thermal structure of the lithosphere. When cooler conditions prevail near the axial region, the lithosphere is thicker and stronger (McNutt 1984; Phipps Morgan and Chen 1993). Conversely, warmer thermal structures produce thinner and weaker lithosphere. Numerical models predict that lithospheric strength and thickness are the main factors that control spacing and throw of normal faults in response to tensional stress (Shaw and Lin 1993; Buck et al. 2005; Behn and Ito 2008). This in turn, will determine abyssal hill dimensions (Escartin et al. 1999; Sauter et al. 2011; Sloan et al. 2012). Cooler, and therefore thicker and stronger lithosphere, is capable of sustaining faults that are spaced further apart and accommodate larger amount of slip, resulting in the formation of broader and taller abyssal hills.

1.3 Influence of Spreading Rate

Spreading rate, which varies from 10 to 150 mm/year, has a dominant influence on abyssal hill morphology (Figs. 1, 2, and 5): Namely, the slower the spreading rate, the taller and wider the abyssal hills become (Malinverno 1991; Goff et al. 1997; Kriner et al. 2006; Goff 2015). This correlation primarily reflects the fact that the slower the spreading rate, the thicker and stronger the lithosphere is within the axial region (see Chapter "Mid-Ocean Ridges"). This thicker and stronger lithosphere is expected to sustain longer-lived faults that will develop larger throw to produce larger abyssal hills. In detail, the relationship between abyssal hill dimensions and spreading rates differs depending on the morphology of the ridge axis (Goff 2015). The correlation is strong for abyssal hills that formed near spreading centers characterized by an axial valley (<70 mm/year), with ultraslow spreading ridges producing the most rugged, highest amplitude abyssal hill relief. But all abyssal hills that formed at spreading centers characterized by an axial high (>70 mm/year) have similar smaller dimensions (Figs. 1, 2, and 5). Abyssal hills formed at intermediate spreading rates (50–90 mm/year), a rate at which the axial morphology transitions between axial valley and axial high, illustrate this dichotomy: At equal spreading rates, smaller abyssal hills are produced where an axial high is present rather than an axial valley (Figs. 1c and 2).

Overall, normal faults account for a small portion of the full spreading rate, with the remainder being accommodated by magmatic accretion of new seafloor within the ~5 km-wide neovolcanic zone. However, as spreading rate decreases, the percentage of extension accommodated by normal faults increases from an estimated ~5% at the fast-spreading East Pacific Rise (Macdonald and Luyendyk 1977; Cowie et al. 1993; Alexander and Macdonald 1996) to about 10% at the

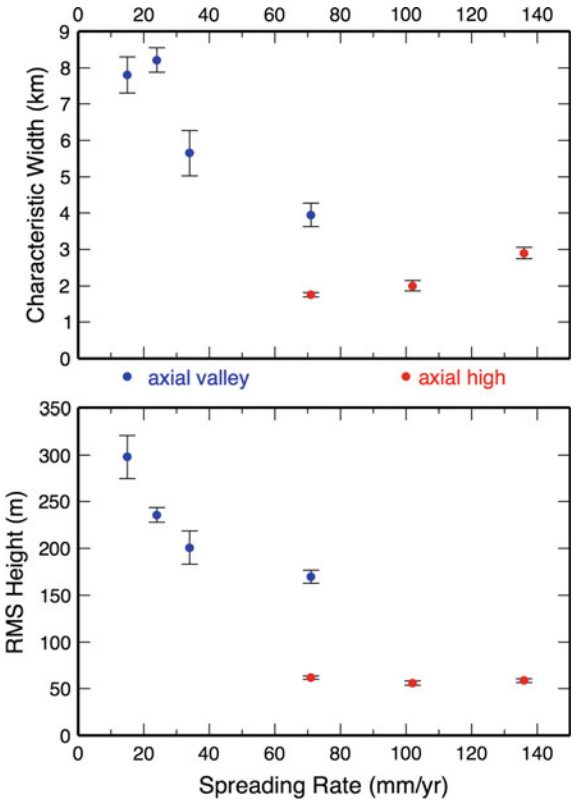

Fig. 5 Relationship between spreading rates and the heights or widths of abyssal hills. Here, the RMS height approximates the average deviation of bathymetry from the mean local depth, and thus corresponds to less than half the average height of the abyssal hills; nonetheless, this parameter objectively evaluates seafloor roughness and applies to all abyssal hills similarly and proportionally. *Blue dots* correspond to spreading centers with a rifted axis, and *red dots* correspond to spreading centers with an axial high. *Error bars* indicate 1 standard deviation. The dimensions of abyssal hills generally decrease with increasing spreading rates. However, abyssal hills formed at spreading centers defined by an axial high display smaller dimensions that remain similar across a broad range of spreading rates (70–140 mm/year). After Goff et al. (1997) and Sloan et al. (2012) (color figure online)

slow-spreading Mid-Atlantic Ridge (Searle et al. 1998a; Escartin et al. 1999). At slow spreading rates, prolonged slip on inward-dipping detachment faults (Figs. 3d and 4b) may occasionally account for most or all of the spreading rate (Cann et al. 1997; Smith et al. 2008; Cannat et al. 2006; Cann et al. 2015). Magma supply at ultraslow spreading rates (<15 mm/year) may become so restricted that lithosphere with little or no extrusive crust is produced for extended periods (>1 Myr), directly exposing mantle on the slip surface of low-angle detachment faults (Cannat et al. 2006;

Sauter et al. 2013). This exposed upper mantle produces an unusually smooth seafloor and, likewise, produces abyssal hills that are strikingly smooth compared to adjacent abyssal hills that expose volcanic rocks (Fig. 4a). In marked contrast, long-lived detachments faults and core complexes have never been reported at fast and ultrafast spreading rates (>90 mm/year). Instead, fast-spreading abyssal hills (Figs. 3a, 3b and 4c) are mostly the product of horst-and-graben tectonics, although volcanic growth faults may mask their true nature in places (Macdonald et al. 1996).

1.4 Influence of Mantle Hot Spots and Cold Spots

Although spreading rate is a general predictor of abyssal hill characteristics, regional thermal anomalies can have an overriding effect. The presence of a hot spot at or near a spreading center creates a warmer thermal structure capable of producing smaller, less rugged abyssal hills than expected. The northern Mid-Atlantic Ridge near the robust Iceland hot spot is a well-known example: Abyssal hills produced along the Reykjanes Ridge south of Iceland display unexpectedly small dimensions that are more akin to those produced at fast spreading centers (Searle et al. 1998b). The opposite effect occurs in areas with anomalously low mantle temperatures (cold spots), such as along the intermediate-spreading Southeast Indian Ridge near the Australian-Antarctic Discordance: There, the ridge axis and the adjacent abyssal hills display all the characteristics of a slow-spreading ridge (Sempéré et al. 1991). The effect of cooler mantle temperatures has also been shown to be the dominant factor controlling the increasingly rougher fabric of abyssal hills along the Southwest Indian Ridge as it approaches the Rodriguez triple junction (Sauter et al. 2011; Sloan et al. 2012). Thus, abyssal hill morphology across the world's ocean records the impact of anomalous mantle temperatures, an impact that may locally dominate that of spreading rates.

1.5 Influence of Ridge Segmentation

The mid-ocean ridge is segmented and offset at intervals by transform faults and by smaller (<30 km) non-transform discontinuities. The off-axis traces of these offsets are pervasive morphologic features on the ridge flanks that interrupt the regular pattern of ridge-parallel abyssal hills, and strongly affect the morphology of abyssal hills terminations.

Transform faults remain stable over long periods of time and create linear fracture zones on the flanks that parallel the spreading direction. Non-transform offsets, on the other hand, tend to migrate along the ridge axis. As a result, their off-axis traces, called discordant zones, often strike obliquely to the ridge. Discordant zones occur symmetrically on both flanks of a ridge axis, producing

V-patterns that point in the direction the discontinuity has been migrating over time (Figs. 6c, d, and 7). The evolving geometry of the spreading axis is thus conveniently recorded in the patterns of fracture zones and discordant zones that are preserved on the ridge flanks (Sloan and Patriat 1992; Cormier et al. 1996).

Spreading rate has a strong influence on the style of non-transform discontinuities, and therefore on the morphology of the discordant zones they create. At slow-spreading rates, non-transform discontinuities offset the axial valley with little or no overlap between ridge segments. The off-axis discordant zones they produce are broad, deep corridors usually containing a series of closed-contour basins (Figs. 1b and 6c). At fast spreading rates, the two offset ridge segments curve toward each other and overlap, enclosing a deep nodal basin between them (Chapter "Mid-Ocean Ridges"; Fig. 6d). This type of non-transform offset is called an overlapping spreading centers, or OSC (Macdonald and Fox 1983). OSCs migrate along the axis, the retreating segment episodically cutting inside of itself and transferring onto one side of the ridge axis the abandoned curved ridge tip and adjacent nodal basin (Fig. 6d). As a result, where OSCs are steadily migrating in one direction, the V-shaped discordant zone consists of a broad zone of curved abandoned ridge tips and intervening nodal basins on one side of the ridge axis,

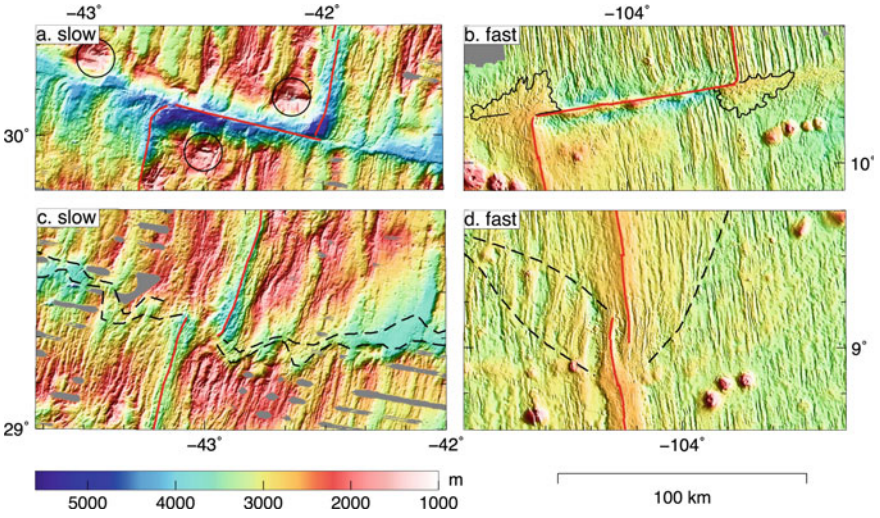

Fig. 6 Varying abyssal hill morphologies in proximity to ridge offsets. *Red lines* mark the plate boundary. **a** Atlantis Transform Fault at the slow-spreading Mid-Atlantic Ridge. *Black circles* outline oceanic core complexes that formed at the inside corner of the ridge-transform intersections; **b** Clipperton transform fault at the fast-spreading East Pacific Rise. *Black lines* highlight the "rooster's combs" that form at some ridge-transform intersections, when magma is injected beyond the segment end and erupts onto the adjacent older plate; **c** non-transform offset at the slow-spreading Mid-Atlantic Ridge. *Dashed lines* outline the off-axis discordant zone and highlight the changing position of this offset through time; **d** OSC at the fast-spreading East Pacific Rise. This non-transform offset has migrated southward, forming a V-shaped discordant zone (*dashed lines*) that points in the direction of migration

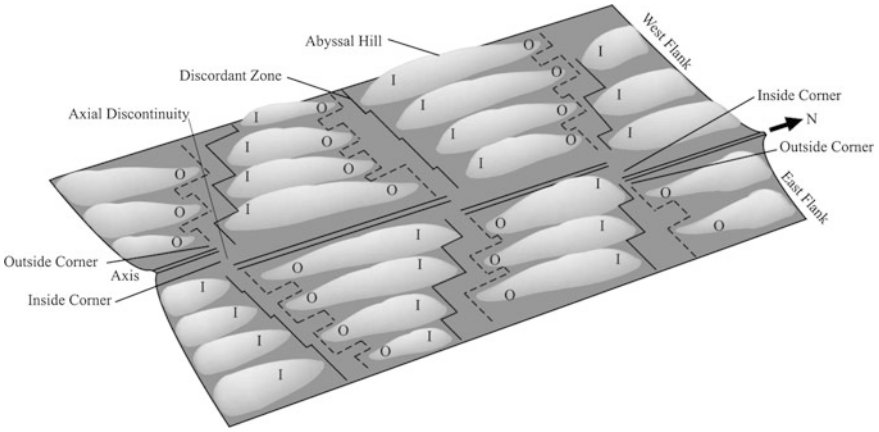

Fig. 7 Schematic of inside corners (*I*) and outside corners (*O*) bathymetry at slow-spreading ridges (Sloan and Patriat, 2004b) (Reprinted from Geochemistry Geophysics Geosystem, 5, Sloan and Patriat, Reconstruction of the flanks of the Mid-Atlantic Ridge, 28° to 29°N: implications for evolution of young oceanic lithosphere at slow-spreading centers, 3, 2004, with permission from John Wiley and Sons). A series of axial segments (*double lines*) generate swaths of abyssal hills separated by discordant zones. Higher abyssal hills form at the inside corners of axial offsets and smaller abyssal hills form near outside corners. This inside corner/outside corner asymmetry is preserved on the ridge flanks, resulting in an asymmetric pattern of abyssal hills terminations: The older seafloor across a discordant zone or a fracture zone is counter-intuitively shallower than the younger side (see also Fig. 6a, c)

while on the other side it consists of a more subtle but well defined lineament separating curved abyssal hills from linear abyssal hills (Wilson 1990).

Ridge offsets also have a marked influence on the morphology of abyssal hill terminations. At slow spreading rates, abyssal hills formed at "inside corners" of a ridge-transform intersection, the corner formed by the ridge axis and the active transform fault, have greater heights and widths than abyssal hills formed at "outside corners", the corner formed by the ridge axis and the inactive fracture zone (Collette 1986; Severinghaus and Macdonald 1988; Sloan and Patriat 2004a) (Fig. 6). This inside-outside corner depth asymmetry is particularly pronounced where high-relief oceanic core complexes have formed at inside corners; core complexes have never been observed to form at outside corners. Such asymmetry is generally ascribed to a contrast in lithospheric coupling across a ridge-transform intersection, whereby newly created seafloor at the inside corner can adjust vertically where it abuts the active plate boundary, but becomes welded to the older, deeper lithosphere across the inactive fracture zone at the outside corner (Severinghaus and Macdonald 1988).

No such consistent depth asymmetry is observed at offsets of the fast spreading ridges. There, magma is sometime injected beyond the end of the ridge segment, through the ridge-transform intersection, and onto the older adjacent lithosphere, the associated volcanism creating a volcanic carapace with lobate edges that

overprints the older abyssal hills (Barth et al. 1994). These features produce subdued ridge-transform intersection highs, which, in map view, have outlines reminiscent of a rooster's comb. The formation of these ridge-transform intersection highs obliterates the trough that developed along the active transform fault and as a result, fracture zones that formed at fast spreading ridges may have a subtle bathymetric expression (Fig. 5a, b).

As the ridge axis approaches a transform fault, it tends to curve toward the segment on the other side of the offset in response to local rotation of the stress field, in the transition from tension to shear (Fox and Gallo 1984; Phipps Morgan and Parmentier 1984; Grindlay and Fox 1993; Croon et al. 2010). Accordingly, at all spreading rates, abyssal hills that form near the outside corners of a ridge-transform intersection echo the shape of the ridge axis and curve towards the offset (Fig. 6a, b). On the other hand, those abyssal hills that formed near the inside corners may display curvature in either direction or no curvature at all. There, strong coupling across the active transform domain may be partially accommodated by distributed strike-slip deformation and result in a curvature in the direction opposite to that of the ridge axis (Sonder and Pockalny 1999; Croon et al. 2010).

2 The Abyssal Plains

As young oceanic lithosphere is rafted away from the mid-ocean ridges, sediments slowly accumulate over the aging and subsiding seafloor and gradually smother the rugged relief of the abyssal hills. The aging lithosphere becomes part of an oceanic basin, these deeper areas delimited by mid-ocean ridges, continental margins, and/or oceanic plateaus (see Chapter "Origin and Geomorphic Characteristics of Ocean Basins"). Deep oceanic basins have water depths ranging between ~3 and ~6 km and constitute ~40% of the World's oceans. Some are thickly sedimented and present a remarkably flat (slope < 0.05°) seafloor known as an abyssal plain. Because abyssal plains are commonly thought of as vast, monotonous submarine deserts, they remain largely under-investigated. Perhaps unexpected features await discovery in these vast, little-explored regions of seafloor.

Two main sedimentary processes deliver sediments to deep oceanic basins: Clastic sedimentation, the delivery of terrigenous material via episodic, fast-moving turbidity currents through the canyons and deep-sea channels that punctuate the continental slopes, and pelagic sedimentation, the slow, steady raining of particulates through the water column (see Chapter "Submarine Canyons and Gullies"). Only one of these two processes, turbidity currents, can generate the flat, sub-horizontal seafloor of the abyssal plains. A turbidity current consists of a slurry of seawater and sediments that is set in motion by earthquakes, tsunamis, or storms. Turbidity currents originate on continental margins and flow far, even on very gentle slopes. The sedimentary deposits they produce, known as turbidites, produce flat, regular sediment layers that may extend far from the continental margins. Where oceanic basins are bounded by passive margins on their landward side,

such as in the Atlantic Ocean or the Antarctic Ocean, turbidity currents can flow unabated by any obstacle and produce smooth abyssal plains over time. However, where oceanic basins are bounded on their landward side by deep subduction trenches, such as around most of the Pacific Ocean, terrigenous sediments carried by turbidity currents become trapped within these trenches and do not reach the adjacent oceanic basins. There, the abyssal hill fabric typically remains visible through the thin drape (<0.5 km) of slowly-accumulating pelagic sediments.

The extreme variability of sediment accumulation in the oceanic basins is well illustrated by the contrasting seafloor fabrics of the Juan de Fuca Plate and that of the Pacific Plate at its western border (Fig. 8). The Juan de Fuca Plate, which is everywhere younger than 10 Ma, is blanketed by up to 2 km of sediments as a result of the exceptionally high rate of terrigenous sediments supplied from North America during the Pleistocene glacial periods (Normark and Reid 2003). In fact, the trench associated with the Cascadia subduction zone is entirely filled with turbidites, with deep sea fans and deep-sea channels extending seaward of the subduction zone, delivering sediments directly to the Cascadia Basin and producing a young, smooth abyssal plain. In stark contrast, the Pacific plate where it approaches the Japan Trench is an order of magnitude older (130–140 Myr), and yet the seafloor still faintly displays its inherited abyssal hill fabric. The comparatively thin ($\sim$500 m) sediment cover for this old seafloor is primarily explained by two factors: this area of the Pacific plate has never drifted through regions with high pelagic sedimentation rates, and only scant terrigenous sediments is supplied from central Japan. In fact, some oceanic basins have never accumulated any significant sediment cover, such as the Southwest Pacific Basin. There, a vast area of seafloor 34–85 Myr-old remains essentially bare of sediments (Rea et al. 2006).

Whether lying beneath the sediments of an abyssal plain or mostly bare of sediments, ancient abyssal hills are reactivated on the outer rise of subduction zones, the area where the subducting plate bends slightly upward and then steeply downward as it approaches the trench (see Chapter "Oceanic Trenches"). Where the abyssal hill fabric is aligned sub-parallel to the subduction zone, the normal faults that define the flanks of abyssal hills are reactivated to accommodate the bending of the plate. Where abyssal hill fabric strikes obliquely to the subduction zone, the plate brakes along a new set of normal faults that strike sub-parallel to the subduction zone (Fig. 8). These new faults appear to be affected by the pre-existing abyssal hill fabric, terminating or stepping-over where they intersect abyssal hills; this geometry suggests that even obliquely striking abyssal hill faults are to some extent reactivated at subduction zones. Thus, at the end of their life cycle, abyssal hills may provide a convenient pathway for seawater to penetrate through the oceanic crust and the lithospheric mantle, possibly leading to the lubrication of the interface between subducting plate and overriding plate. Their reactivation may thus facilitate the input of water in the mantle wedge above the subducting plate, enhancing arc volcanism and possibly leading to serpentinization in the upper mantle.

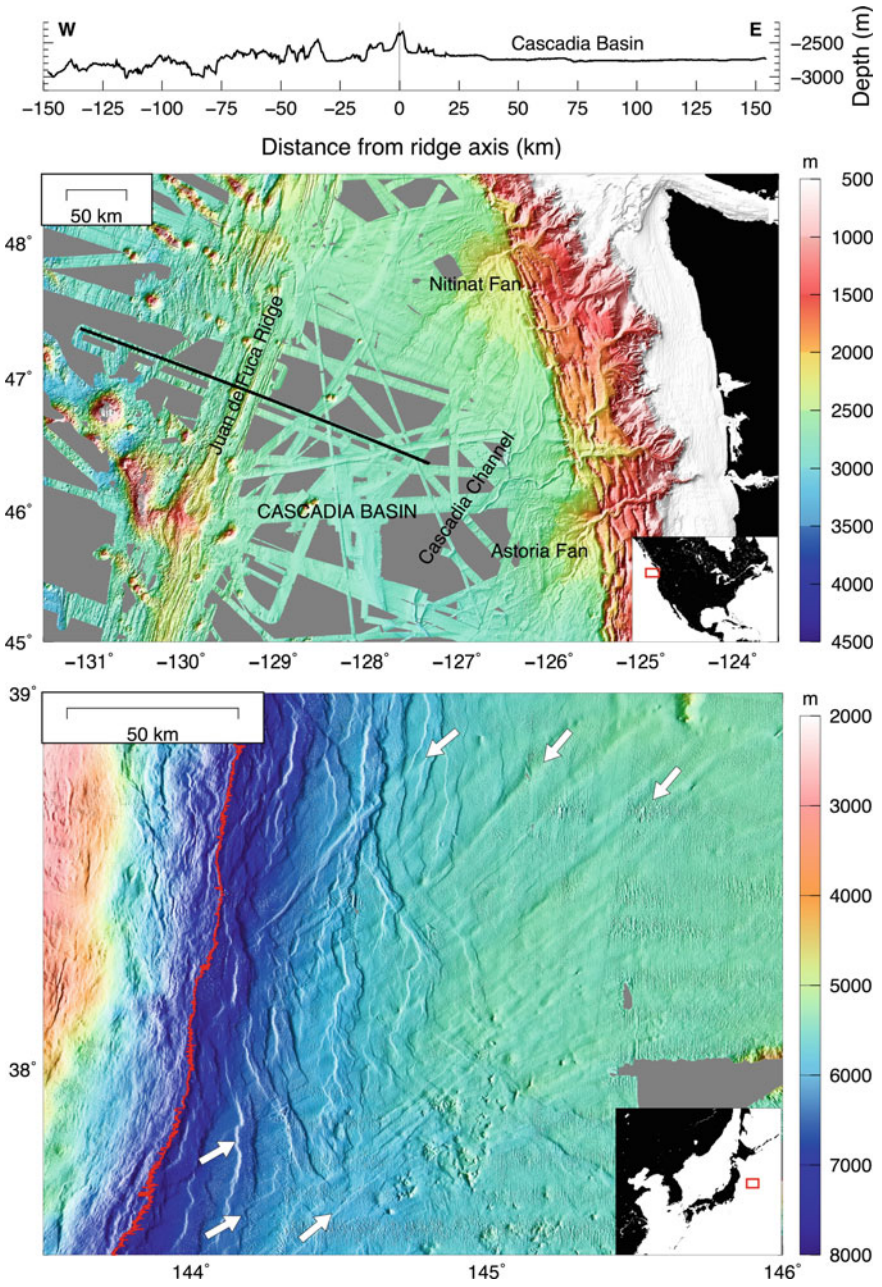
W
E
Cascadia Basin
−2500
−3000
Depth (m)
−150 −125 −100 −75 −50 −25 0 25 50 75 100 125 150
Distance from ridge axis (km)
50 km
m
500
1000
1500
2000
2500
3000
3500
4000
4500
48°
47°
46°
45°
Nitinat Fan
Juan de Fuca Ridge
CASCADIA BASIN
Cascadia Channel
Astoria Fan
−131° −130° −129° −128° −127° −126° −125° −124°
39°
38°
50 km
m
2000
3000
4000
5000
6000
7000
8000
144° 145° 146°

◂**Fig. 8** Abyssal hills and abyssal plains near the end of their life cycle at two contrasting subduction zones; insets locate the displayed areas. *Top map* Bathymetry of the Juan de Fuca Ridge and Juan de Fuca Plate off the west coast of North America. An exceptionally high sedimentation rate completely obscures subduction trench and abyssal hills. The *black line* locates the bathymetric profile shown above to illustrate the flat bathymetry of the Cascadia Basin. *Bottom map* Bathymetry of the Pacific plate off the Japan Trench (Fujiwara et al. 2011). Some of the world's oldest seafloor (~140 Myr) is subducting beneath Japan and yet, the abyssal hill fabric (*white arrows*) remains visible through the relatively thin sediment cover. A new set of normal faults oriented sub-parallel to the trench axis (*red*) cross-cuts the pre-existing fabric of the abyssal hills to accommodate the bending of the subducting plate

3 Some Outstanding Questions

Developments in deep-submergence and marine geophysical technology over the past few decades have lead to a much improved characterization of abyssal hills. Yet, many questions regarding their formation and evolution remain either unanswered or debatable. Some are listed below.

3.1 What Is the Width of the Plate Boundary Zone at Mid-Ocean Ridges?

The distance over which abyssal hills continue to grow, and thus the distance over which lithospheric deformation accumulates, is a direct measurement of the width of plate boundary zone. The documented growth of abyssal hills out to at least 35 km from the ridge axis (see Sect. 1.1) indicates that the plate boundary zone is at minimum 70 km wide. However, data are lacking that could test some follow-up questions, such as: What is the maximum extent of the plate boundary zone? How does the width of the plate boundary zone depend (or not) on spreading rates, patterns of axial segmentation, or regional variations in the thermal structure of the lithosphere?

At two slowly-diverging plate boundaries on land, in Iceland and along the Afar Rift in Ethiopia, geodetic investigations indicate deformation zones as wide as 100–150 km (Wright et al. 2012). However, underwater geodesy is still an emerging technology and the true extent of the deformation zone at submerged mid-ocean ridges remains to be quantified. Alternative and/or complementary methods that could contribute useful evidence include: (1) the acquisition of high-resolution bathymetric data that extend as far as 100–150 km to either side of various mid-ocean ridges, presumably encompassing the entire plate boundary zone; (2) the acquisition of high-resolution seismic reflection profiles where sediments accumulate sufficiently fast to record the full history of tectonic deformation in their stratigraphy; (3) the long-term deployment of arrays of ocean bottom seismometers across the plate boundary zone in order to determine the width of the zone of background seismicity.

3.2 Do Abyssal Hills Offer Long-Lived Pathways for Fluids Through the Oceanic Crust?

Various observations, including fossil hydrothermal sites and enhanced heat flow measurements, suggest that the faults bounding the abyssal hills may favor hydrothermal circulation off-axis (Abbott et al. 1992; Haymon et al. 2005). If fluid circulation continued to focus along the flanks of abyssal hills long after they become buried under a thick sediment cover, this process may be expressed in the sedimented seafloor as clusters of dissolution structures or pockmarks that align with the trend of the buried abyssal hills. More extensive investigation of the vast abyssal plains using high-resolution multibeam bathymetric and sidescan sonars should record the subtle expression of such features, if present.

3.3 How Does Mass Wasting Affect Abyssal Hill Morphology?

Talus is commonly observed at the base of young abyssal hills and landslide scars have been mapped along the walls of rift valleys and transform faults (Mitchell et al. 2000; Cannat et al. 2013). However, it remains unclear whether fresh talus or landslides only occur where faults are recently active, or whether they can also be indicative of slope instability and the progressive erosion of abyssal hill flanks. Detailed geophysical and near-bottom investigations that extend beyond the broader plate boundary zone may provide an answer.

3.4 Are the Abyssal Plains as Featureless as We Think?

The abyssal plains remain largely unexplored: Do subtle features occur across their vast expanses that have escaped detection? For example, does low-level fluid circulation lead to the formation of pockmarks or dissolutions structures across the abyssal plain? Recent investigations suggest that turbidity currents may evolve into erosional debris flows capable of crossing the flat abyssal plain (Talling et al. 2007): Do such events leave characteristic signatures on the seafloor? Are rare, large magnitude intraplate earthquakes producing liquefaction features equivalent to the clusters of sand blows observed on land, or some subtle fault scarps and fissures? The morphological signature of volcanism related to hotspots is obvious, but how common are the “petit-spot” volcanoes that erupt on subducting plates seaward of trenches in response to plate flexure, as characterized by Hirano et al. (2006)?

Acknowledgements We are grateful for the public availability of multibeam bathymetric data through the National Geophysical Data Center (https://www.ngdc.noaa.gov/mgg/bathymetry/multibeam.html) and GeoMapapp (http://www.geomapapp.org). These bathymetric data have been processed with MB-System and all figures have been generated with GMT, both freely available software (Caress et al. 2015; Wessel et al. 2013). We thank D. Sauter for the gridded bathymetric data of the Southwest Indian Ridge, T. Fujiwara for the gridded bathymetric data of the Japan Trench, a dataset compiled by the Japan Oceanographic Data Center and JAMSTEC, and D.K. Blackman for review.

References

Abbott DH, Stein CA, Diachuk O (1992) Topographic relief and sediment thickness: their effects on the thermal evolution of the oceanic crust. Geophys Res Lett 19:1975–1978

Alexander RT, Macdonald KC (1996) Sea Beam, SeaMARC II, and Alvin- based studies of faulting on the East Pacific Rise 9°20′–9°50′N. Mar Geophys Res 18:557–587

Barth GA, Kastens KA, Klein E (1994) The origin of bathymetric highs at ridge-transform intersections: a multi-disciplinary case study at the Clipperton Fracture Zone. Mar Geophys Res 16:1–50

Behn MD, Ito G (2008) Magmatic and tectonic extension at mid-ocean ridges: 1. Controls on fault characteristics. Geochem Geophys Geosyst. doi:10.1029/2008GC001965

Buck WR, Lavier LL, Poliakov ANB (2005) Modes of faulting at mid-ocean ridges. Nature 434:719–723

Cann JR, Blackman DK, Smith DK, McAllister E, Janssen B, Mello SLM, Avgerinos A, Pascoe AR, Escartin J (1997) Corrugated slip surfaces formed at ridge-transform intersections on the Mid-Atlantic Ridge. Nature 385:329–332

Cann JR, Smith DK, Escartin J, Schouten H (2015) Tectonic evolution of 200 km of Mid-Atlantic Ridge over 10 million years—interplay of volcanism and faulting. Geochem Geophys Geosyst. doi:10.1002/2015GC005797

Cannat M, Sauter D, Mendel V, Ruellan E, Okino K, Escartin J, Combier V, Baala M (2006) Modes of seafloor generation at a melt-poor ultraslow-spreading ridge. Geology 34:605–608

Cannat M, Mangeney A, Ondréas H, Fouquet Y, Normand A (2013) High resolution bathymetry reveals contrasting landslide activity shaping the walls of the Mid-Atlantic Ridge axial valley. Geochem Geophys Geosyst 14:996–1011

Cochran JR, Sempéré J-C, The SEIR Scientific Team (1997) The Southeast Indian Ridge between 88°E and 120°E: Gravity anomalies and crustal accretion at intermediate spreading rates. J Geophys Res 102(B7):15463–15487. doi:10.1029/97JB00511

Collette BJ (1986) Fracture zones in the North Atlantic: morphology and a model. J Geol Soc 143:763–774

Cormier MH, Scheirer DS, Macdonald KC (1996) Evolution of the East Pacific Rise at 16°-19°S since 5 Ma: bisection of overlapping spreading centers by new, rapidly migrating propagating ridge segments. Mar Geophys Res 18:53–84

Cowie PA, Scholtz CH, Edwards MH, Malinverno A (1993) Fault strain and seismic coupling on mid-ocean ridges. J Geophys Res 98:17911–17920

Croon MB, Cande SC, Stock JM (2010) Abyssal hill deflections at Pacific-Antarctic ridge-transform intersections. Geochem Geophys Geosyst doi:10.1029/2010GC003236

Caress DW, Chayes DN, dos Santos Ferreira, C (2015) MB-system seafloor mapping software—processing and display of swath sonar data. http://www.mbari.org/data/mbsystem

Escartín J, Cowie PA, Searle RC, Allerton S, Mitchell NC, MacLeod CJ, Slootweg AP (1999) Quantifying tectonic strain and magmatic accretion at a slow spreading ridge segment, Mid-Atlantic Ridge, 29°N. J Geophys Res 104(B5):10421–10437

Fox PJ, Gallo DG (1984) A tectonic model for ridge-transform-ridge plate boundaries: implications for the structure of oceanic lithosphere. Tectonophysics 104:205–242
Fujiwara T, Kodaira S, No T, Kaiho Y, Takahashi N, Kaneda Y (2011) The 2011 Tohoku-Oki earthquake: displacement reaching the trench axis. Science 334:1240
Goff JA (1991) A global and regional stochastic analysis of near-ridge abyssal hill morphology. J Geophys Res 96:21, 713–21,737. doi:10.1029/91JB02275
Goff JA (1992) Quantitative characterization of the abyssal hill morphology along flow lines in the Atlantic Ocean. J Geophys Res 97:9183–9202
Goff JA (2015) Comments on "Glacial cycles drive variations in the production of oceanic crust". Science 349:1065a
Goff JA, Tucholke BE, Lin J, Jaroslow GE, Kleinrock MC (1995) Quantitative analysis of abyssal hills in the Atlantic Ocean: a correlation between axis crustal thickness and extensional faulting. J Geophys Res 100:22509–22522. doi:10.1029/95JB02510
Goff JA, Ma Y, Shah AK, Cochran JR, Sempéré J-C (1997) Stochastic analysis of seafloor morphology on the flank of the Southeast Indian Ridge: the influence of ridge morphology on the formation of abyssal hills. J Geophys Res 102:15521–15534
Goff JA, Smith WHF, Marks KM (2004) The contributions of abyssal hills morphology and noise to altimetric gravity fabric. Oceanography 17:24–37
Grindlay NR, Fox PJ (1993) Lithospheric stresses associated with nontransform offsets of the Mid-Atlantic Ridge: implications from a finite element analysis. Tectonics 12:982–1003
Haymon RM, Macdonald KC, Benjamin SB, Ehrhardt CJ (2005) Manifestations of hydrothermal discharge from young abyssal hills on the fast-spreading East Pacific Rise flank. Geology 33:153–156
Heezen BC, Tharp M, Ewing M (1959) The floors of the oceans: I. The North Atlantic. Geological Society of America, Special Paper vol 65, p 126
Hirano N, Takahashi E, Yamamoto J, Abe N, Ingle SP, Kaneoka I, Hirata T, Kimura JI, Ishii T, Ogawa Y, Machida S, Suyehiro K (2006) Volcanism in response to plate flexure. Science 313:1426–1428
Kriner K, Pockalny RA, Larson RL (2006) Bathymetric gradients of lineated abyssal hills: inferring seafloor spreading vectors and a new model for hills formed at ultra-fast rates. Earth Planet Sci Lett 242:98–110
Lonsdale P (1977) Structural geomorphology of a fast-spreading rise crest: the East Pacific Rise near 3°25′S. Mar Geophys Res 3:251–293
Luyendyk B (1970) Origin and history of abyssal hills in the northeast Pacific. Geol Soc Am Bull 81:2237–2260
Macdonald KC (1982) Mid-ocean ridges: fine scale tectonic, volcanic and hydrothermal processes within the plate boundary zone. Annu Rev Earth Planet Sci 10:155–190
Macdonald KC, Fox PJ (1983) Overlapping spreading centers: new accretion geometry on the East Pacific Rise. Nature 302:55–58
Macdonald KC, Luyendyk BP (1977) Deep-Tow studies of the structure of the Mid-Atlantic Ridge crest near lat 37°N. Geol Soc Am Bull 88:621–636
Macdonald KC, Luyendyk BP (1985) Investigation of faulting and abyssal hill formation on the flanks of the East Pacific Rise (21°N) using ALVIN. Mar Geophys Res 7:515–535
Macdonald KC, Fox PJ, Alexander RT, Pockalny R, Gente P (1996) Volcanic growth faults and the origin of Pacific abyssal hills. Nature 380:125–129
MacLeod CJ, Searle RC, Murton BJ, Casey JF, Mallows C, Unsworth SC, Achenbach KL, Harris M (2009) Life cycle of oceanic core complexes. Earth Planet Sci Lett 287:333–344
Malinverno A (1991) Inverse square-root dependence of mid-ocean ridge flank roughness on spreading rate. Nature 352:58–60
McNutt M (1984) Lithospheric flexure and thermal anomalies. J Geophys Res 89:11180–11194
Menard HW (1964) Marine geology of the Pacific. McGraw Hill, New York
Mitchell NC, Tivey MA, Gente P (2000) Seafloor slopes at mid-ocean ridges from submersible observations and implications for interpreting geology from seafloor topography. Earth Planet Sci Lett 183:543–555

Normark WR, Reid JA (2003) Extensive deposits on the Pacific plate from late Pleistocene North American glacial lake outbursts. J. Geology 111:617–637
Olive JA, Behn MD, Ito GT, Buck WR, Escartín J, Howell S (2015) Sensitivity of seafloor bathymetry to climate-driven fluctuations in mid-ocean ridge magma supply. Science 350:310–313
Phipps Morgan J, Chen YJ (1993) Dependence of ridge-axis morphology on magma supply and spreading rate. Nature 364:706–708
Phipps Morgan J, Parmentier EM (1984) Lithospheric stress near a ridge-transform inter-section. Geophys Res Lett 11:113–116
Rea DK (1975) Model for the formation of topographic features of the East Pacific Rise crest. Geology 3:77–80
Rea DK, Lyle MW, Liberty LM, Hovan SA, Bolyn MP, Gleason JD, Hendy IL, Latimer JC, Murphy BM, Paul CF, Rea THC, Stancin AM, Thomas DJ (2006) Broad region of no sediment in the southwest Pacific Basin. Geology 34:873–876
Sauter D, Sloan H, Cannat M, Goff J, Patriat P, Schaming M, Roest WR (2011) From slow to ultra-slow: how does spreading rate affect seafloor roughness and crustal thickness? Geology 39:911–914. doi:10.1130/G32028
Sauter D, Cannat M, Rouméjon S, Andreani M, Birot D, Bronner A, Brunelli D, Carlut J, Delacour A, Guyader V, MacLeod CJ, Manatschal G, Mendel V, Ménez B, Pasini V, Ruellan E, Searle R (2013) Continuous exhumation of mantle-derived rocks at the Southwest Indian Ridge for 11 million years. Nat Geosci 6:314–320
Searle RC (1984) GLORIA survey of the East Pacific Rise near 3.5°S: tectonic and volcanic characteristics of a fast spreading mid-ocean rise. Tectonophysics 101:319–344
Searle RC, Cowie PA, Mitchell NC, Allerton S, MacLeod CJ, Escartin J, Russell SM, Slootweg PA, Tanaka T (1998a) Fault structure and detailed evolution of a slow spreading ridge segment: the Mid-Atlantic Ridge at 29°N. Earth Planet Sci Lett 154:167–183
Searle RC, Keeton JA, Owens RB, White RS, Mecklenburgh R, Parsons B, Lee S-M (1998b) The Reykjanes Ridge: structure and tectonics of a hot-spot influences, slow-spreading ridge, from multibeam bathymetry, gravity and magnetic investigations. Earth Planet Sci Lett 160:463–478
Sempéré J-C, Palmer J, Christie DM, Phipps Morgan J, Shor AN (1991) The Australian-Antarctic discordance. Geology 19:429–432
Severinghaus JP, Macdonald KC (1988) High inside corners at ridge-transform intersections. Mar Geophys Res 9:353–367
Shaw PR, Lin J (1993) Causes and consequences of variations in faulting style at the Mid-Atlantic Ridge. J Geophys Res 98:21839–21851
Sloan H, Patriat P (1992) Kinematics of the North American-African plate boundary between 28° and 29°N during the last 10 Ma: evolution of the axial geometry and spreading rate and direction. Earth Planet Sci Lett 113:323–341
Sloan H, Patriat P (2004a) Generation of morphotectonic fabric on the Mid-Atlantic Ridge flanks, 28° to 29°N: Implications for the limits of tectonic deformation and abyssal hill formation. Geochem Geophys Geosyst 5. doi:10:1029/2004GC000584
Sloan H, Patriat P (2004b) Reconstruction of the flanks of the Mid-Atlantic Ridge, 28° to 29°N: Implications for evolution of young oceanic lithosphere at slow-spreading centers. Geochem Geophys Geosyst 5. doi:10.1029/2004GC000727
Sloan H, Sauter D, Goff JA, Cannat M (2012) Abyssal hill characterization at the ultraslow spreading Southwest Indian Ridge. Geochem Geophys Geosyst 13. doi:10.1029/2011GC003850
Smith DK, Escartín J, Cannat M, Tolstoy M, Fox CG, Bohnenstiehl DR, Bazin S (2003) Spatial and temporal distribution of seismicity along the northern Mid-Atlantic Ridge (15°–35°N). J Geophys Res 108 doi:10.1029/2002JB001964
Smith DK, Escartín J, Schouten H, Johnson JR (2008) Fault rotation and core complex formation: Significant processes in seafloor formation at slow-spreading mid-ocean ridges (Mid-Atlantic Ridge, 13°–15°N). Geochem Geophys Geosyst 9. doi:10.1029/2007GC001699

Sonder LJ, Pockalny RA (1999) Anomalously rotated abyssal hills along active transforms: distributed deformation of oceanic lithosphere. Geology 27:1003–1006

Talling PJ, Wynn RB, Masson DG, Frenz M, Cronin BT, Schiebel R, Akhmetzhanov AM, Dallmeier-Tiessen S, Benetti S, Weaver PPE, Georgiopoulou A, Zühlsdorff C, Amy LA (2007) Onset of submarine debris flow deposition far from original giant landslide. Nature 450:541–544

Wessel P, Smith WHF, Scharroo R, Luis JF, Wobbe F (2013) Generic mapping tools: improved version released. EOS Trans AGU 94(45):409–410. doi:10.1002/2013EO450001

Wilson DS (1990) Kinematics of overlapping rift propagation with cyclic rift failure. Earth Planet Sci Lett 96:384–392

Wright TJ, Sigmundsson F, Pagli C, Belachew M, Hamling IJ, Brandsdottir B, Keir D, Pedersen R, Ayele A, Ebinger CJ, Einarsson P, Lewi E, Calais E (2012) Geophysical constraints on the dynamics of spreading centers from rifting episodes on land. Nat Geosci 5:242–250